ELSEVIER

Electroencephalography and clinical Neurophysiology 108 (1998) 299–305

Topography and morphology of heart action-related EEG potentials

G. Dirlich*, T. Dietl, L. Vogl, F. Strian

Max Planck Institute of Psychiatry, Kraepelinstrasse 10, 80804 Munich, Germany

Accepted for publication: 20 December 1997

Abstract

Joint ECG and EEG measurements were performed in 22 healthy subjects under standardized laboratory conditions. Averaged EEG potentials were computed using the R-peaks in the ECG as reference events. Spatio-temporal potential patterns of heart action-related EEG activity were obtained from 26 scalp channels. A heart action-related positive potential was found, peaking over the parietal scalp regions. Its independence from the cardiac electrical field, the source of an EEG artifact that may be confounded with heart action-related brain potentials, is demonstrated. The potential reaches its maximum amplitude of about 0.5 μV at a latency of about 500 ms after the R-peak. Its topography, with peak amplitudes at the parietal electrode locations, is different from the topography of potentials observed in the few comparable experimental studies published so far. This suggests the presence of somatosensory-evoked components in heart action-related potentials and indicates that a renewed discussion of the underlying neuronal processes is necessary. © 1998 Elsevier Science Ireland Ltd.

Keywords: Heart action-related potential; Somatosensory evoked potential; Viscerosensory afferences; Heart-beat perception

1. Introduction

The recurrent action of the heart and the subsequent pulsatile vascular events are the source of a variety of afferent neuronal signals. Those with well-known physiological significance are the visceral signals contributing to the autonomous cardiovascular control originating from intra-cardial, carotid sinus and aortic arch baroreceptors (Cervero and Foreman, 1990; Jänig, 1996). Other signals originate from the 'seismic activity' in the body caused by the heart action and the consequent pulse wave, i.e. they originate from the mechanical impact of the heart action and pulse wave on somatosensorily-innervated tissue (Paintal, 1972). Somatosensory mechanoreceptors in the chest may pick up the cyclical impact of the heart muscle on the surrounding tissue and mechanoreceptors located near the large arteries are stimulated by small translocations of tissues induced by the pulse wave. Events and signals of this kind may constitute the basis for the perception of palpitations associated with the beating of the heart (Jones et al., 1987; Reed et al., 1990). All these signals originating at different locations in the body and at different latencies with respect to the heart action form a shower that recurs synchronously with each heart action.

In order to detect the EEG effects of these signals, a number of experimental studies based on an event-related potential (ERP) approach have been performed by several research groups (Chen and Dworkin, 1982; Jones et al., 1986, 1988; Schandry et al., 1986; Riordan et al., 1990; Montoya et al., 1993; Schandry and Montoya, 1996). The reported findings on scalp potentials obtained by R-peak-related EEG averaging have been inconsistent. Schandry et al. (1986), Montoya et al. (1993) and Schandry and Montoya (1996) described a positive potential over the frontal scalp regions at a latency of 350–450 ms. However, the findings of Jones et al. (Jones et al., 1986, 1988) and Riordan et al. (1990), although preliminary, were not in accordance with Schandry's and Montoya's data with respect to topography and morphology.

Different hypotheses for the generation of the observed potentials have been suggested. Jones et al. (1986, 1988) and Riordan et al. (1990) hypothesized that the cyclical mechanical impact of the heart on the chest wall may be the explanation for the heart-beat sensation. This would

* Corresponding author. Tel.: +49 089 30622226; fax: +49 089 30622605.

PII S0168-5597(98)00003-3

EEP 97729

require the transmission of neuronal signals to the cortex along somatosensory pathways. Schandry and Montoya (1996) proposed a contrasting hypothesis. As they had observed a potential over the frontal brain regions rather than over the somatosensory projection areas, they hypothesized a transmission of the underlying signals along visceral pathways to fronto-cortical areas.

All these studies applied the method of event-related EEG averaging using the R-peak of the ECG as the reference event. This approach is based on an analogy between potentials evoked by experimental sensory stimuli and heart action-evoked potentials. There is, however, an important difference between the two potentials. The basic assumption of stimulus-related EEG averaging is that all events that can elicit potentials and that are not reference events occur in asynchronous, random-like temporal relation to the reference events. Therefore, their effects on the EEG can be canceled out by averaging over extended periods of time. This is not the case in R-peak-related EEG averaging. Potential components caused by non-brain electric factors recurring phase-locked with the heart action are extracted from the EEG together with the brain electric components. Both types of components are superimposed in the measured and averaged scalp potentials and are computationally inseparable.

The largest non-brain electric component is caused by the cardiac electrical field. The 'cardiac field artifact' (CFA) is most prominent during the segment of the cardiac cycle corresponding to the PQRST complex of the ECG. Here, it masks or mimics heartbeat-related brain potential components. Although the importance of the CFA in heart action-related averaged EEG potentials has been recognized in the studies mentioned above, convincing evidence that the described potentials represent brain electric processes undistorted by artifacts is still lacking.

We have recently investigated the CFA and demonstrated that during an ECG-dependent segment of the cardiac cycle, between the end of the T-wave and the onset of the next P-wave, the strength of the cardiac field is negligible. During this 'low-CFA segment' an almost undisturbed measurement of heart action-related potentials is possible (Dirlich et al., 1997). In addition to this window, another very small window can be found during the strongly CFA-contaminated ST-interval (near the J-point of the ECG) where the cardiac field has almost completely decayed and before it begins to build up again. An additional snapshot-like measurement of the potentials is also possible here.

The present study utilizes these conditions in the search for heart action-related potentials. The search is focused on the low-CFA segments of the cardiac cycle. Despite minor methodological differences between our study and the above-mentioned studies, we had expected to be able to confirm the published findings on the topography and morphology of the heartbeat-related potentials. However, unexpectedly, our observational data were not consistent with the previously-reported findings.

2. Methods

Two groups of healthy subjects were investigated in the two-part study. Twelve men aged 21–33 years participated in part 1. Ten adults (5 male, 5 female, aged 20–35 years) participated in part 2. The subjects were not preselected with respect to their ability to perceive their heartbeat. Prior to the experiments the subjects were informed about the purpose of the study and the experimental protocol. They were paid for their participation.

The experiments took place in an electrically- and sound-shielded laboratory. The subjects were seated in a chair with an almost vertical back support. Prior to the start of the recording of data they found a comfortable position with both feet on the ground and both forearms on the arm rests. The subjects were instructed to watch a silent movie on a television set 2 m in front of them during the entire recording time. In particular, they were asked to always keep their heads in the same orientation to the TV screen and in a constant relationship to the body trunk. This was checked throughout the recording time so that uncontrolled effects of the cardiac electrical field were reduced. These conditions had a twofold purpose: first, to reduce the frequency of eye movements, and second, to distract the subjects from observing their heartbeats.

With the exception of an additional stimulation condition in part 2, the experimental conditions were identical in both parts of the study. This additional condition consisted of repetitive electrostimuli applied to the left index finger at a frequency of 0.9 Hz. The purpose of part 2 of the study was to explore the extraction of somatosensory evoked potentials and heart action-related potentials from the same EEG data. Only the findings on the heart action-related potentials are reported here.

In part 1 of the study, data were recorded in 4 blocks, each of 400 s duration. In part 2, 8 blocks of 360 s duration were recorded. Breaks of 30 s separated the blocks in both parts of the study. The recordings were completed within 35 (part 1) and 60 (part 2) min.

The ECG was recorded from two limb leads, the right arm and the left leg, and 4 ECG chest leads, with electrodes positioned at the 5th intercostal space at the midaxillary line, on the right and left sides of the chest, and at the level of the 5th midspinal line. Twenty-six EEG channels were set up according to the augmented 10–20 system (Jasper, 1958). Data were collected by a DC 32 channel recording system (Schwind Medizintechnik, Erlangen, Germany) at a sampling rate of 500 Hz. The amplitude resolution was 0.3 mV.

The difference between the two limb lead signals was used for the R-peak detection. Three geometrically-orthogonal components of the cardiac electrical field, the lateral, the vertical and the sagittal, were computed: C_{lat} (the difference between the two midaxillary leads), C_{ver} (the average of the 4 chest leads with Cz as common reference), and C_{sag} (the difference between the midsternal and midspinal leads).

Cz-referenced EEG channels were computationally re-referenced with the average of the two earlobe-electrodes as reference. This reference is comparable with the linked mastoids reference used in the above-mentioned studies (e.g. Schandry and Montoya, 1996).

The recorded data were visually screened for artifacts, namely movement, muscular and DC-drift artifacts. Epochs with artifacts were excluded from the analysis. Eyeblink artifacts were detected and corrected computationally (Gratton et al., 1983).

For the averaging procedure, sweeps were defined as starting 300 ms before the R-peak, i.e. about 50 ms before the onset of the P-wave, and ending 1200 ms after the R-peak.

From the data of the 12 subjects in part 1, a grand average (GA1) was computed. Analogously, a grand average (GA2) was computed from the data of the 10 subjects in part 2. Time-courses and brain maps shown in the figures depict these grand average (GA) data.

In addition to the GA, individual analyses of the potentials of all subjects were also carried out. First, the low-CFA segments were determined from the averaged ECG. Two time points, $t1$ and $t2$, were arbitrarily chosen in the post-T-wave segment of the cardiac cycle. The 3 orthogonal components of the cardiac field, C_{lat}, C_{ver} and C_{sag} were determined for both time points, $t1$ and $t2$. The magnitude of the differences δ ($t2$, $t1$) of the 3 cardiac field components between $t1$ and $t2$ was estimated by

$$\delta(t2,\ t1) = \sqrt{(C_{lat}(t2) - C_{lat}(t1))^2 + (C_{ver}(t2) - C_{ver}(t1))^2 + (C_{sag}(t2) - C_{sag}(t1))^2}.$$

Then, moving $t1$ towards the end of the T-wave and $t2$ towards the beginning of the consecutive P-wave as long as δ ($t2$, $t1$) < 50 μV, the limits of the low-CFA segments were estimated (this implies that at any time during the low-CFA segment the changes of the field strength in any of the 3 spatial directions do not exceed 50 μV). Analogously, a time-point $t0$ near the J-point of the ECG was selected so that δ ($t1$, $t0$) < 50 μV.

Four sampling points s0, s1, s2, and s3 were selected: s0 at $t0$, s1 near $t1$, s2 near the peak of the GA1 potential in channel Pz and s3 near the end of the low-CFA segment of GA1.

Measurements of two transient amplitudes were taken between the sampling points s2–s0 and s1–s0. These data, forming two samples of differences of amplitudes for each of the 26 channels were statistically treated by the Wilcoxon test for two matched samples.

3. Results

Each of the 12 subjects in part 1 of the study contributed about 2000 cardiac cycles, i.e. sweeps to the GA1 data (Figs. 1 and 2). In the lower parts of these figures the time-courses

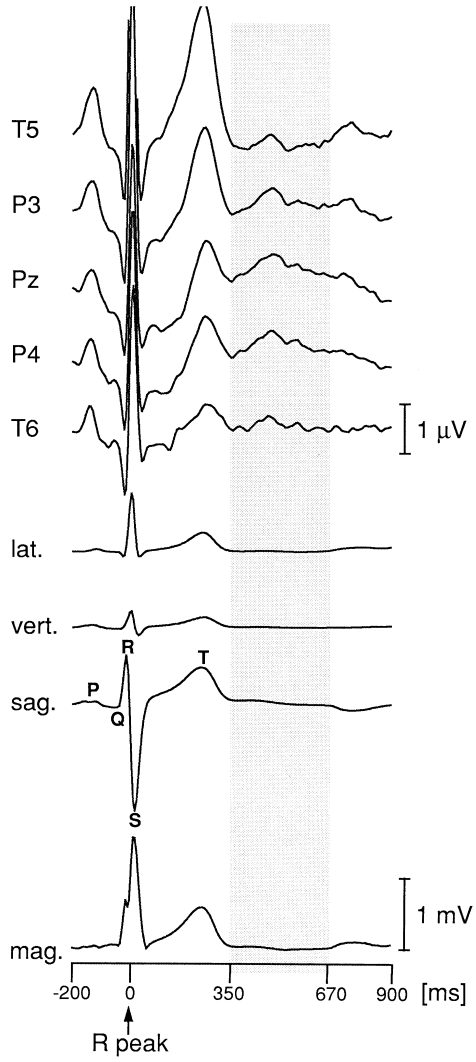

Fig. 1. Grand average, GA1, of scalp potentials (top: channels T5, P3, Pz, P4, T6); cardiac electrical field components (center: lateral, vertical, sagittal) and cardiac field magnitude (bottom). Reference event is the ECG R-peak. The shaded area marks the time-interval shown in Fig. 2 at greater time and amplitude resolution.

of the 3 orthogonal cardiac field components (C_{lat}, C_{ver} and C_{sag}) and the magnitude of the cardiac electrical field strength demonstrate the field at chest level during a segment of the cardiac cycle beginning 200 ms before the R-peak and ending 900 ms after the R-peak. The amplitude range during this time-interval is about 1000 μV.

In contrast to the marked amplitudes during the PQRST segment of the cardiac cycle, only very much smaller amplitudes in the 'post-T-wave to pre-P-wave' interval can be seen (shaded areas in Figs. 1 and 2). For the GA1, the low-CFA criterion, i.e. differences in the field magnitude not exceeding 50 μV, holds for the interval beginning 350 ms after and ending 650 ms after the R-peak. The individual determination of the low-CFA segments was possible for all subjects, yielding the sampling points s0, s1 and s2 (Table 1).

The shaded area in Fig. 1 demonstrates the positioning of

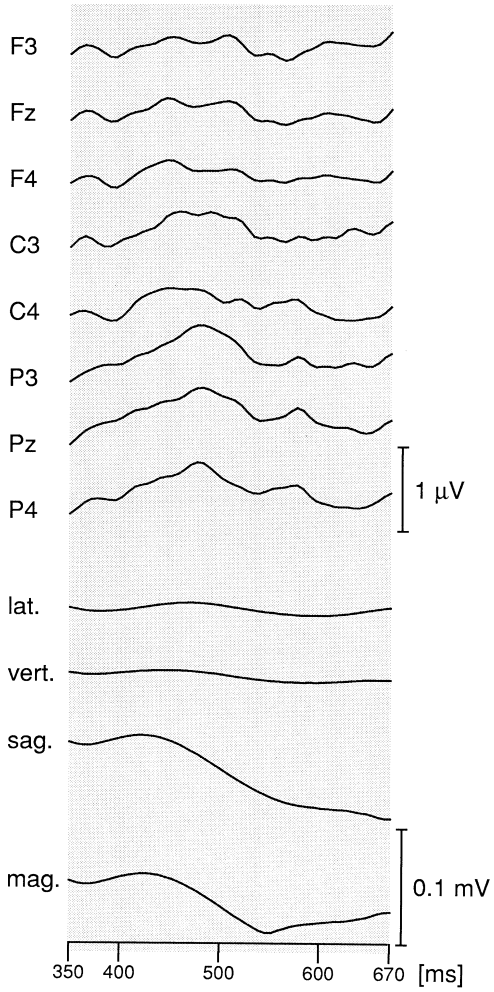

Fig. 2. Grand average, GA1, of scalp potentials and cardiac field descriptors (shaded area corresponds to that in Fig. 1 but with greater time and amplitude resolution). The amplitude enhancement for the scalp channels is 2.0 and for the cardiac field descriptors 10.0 in relation to Fig. 1.

the low-CFA segment within the cardiac cycle. The sampling points s1, s2 and s3 lie inside this interval, shown in enhanced time and amplitude resolution in Fig. 2. A comparison of the magnitude of the cardiac field at the R-peak (about 1400 μV) and the range during the interval 350–650 ms (about 40 μV) shows that the field strength has decayed to less than 3% of its strength observed at the R-peak. An estimation of the possible effects from the residual cardiac field at the scalp electrode locations during the low-CFA segment can be based on the description of the CFA in Dirlich et al. (1997): the effects do not exceed 1% of the amplitudes measured at thorax locations. For example, the magnitude of the cardiac field at the peak of the T-wave is 395 μV for GA1. The respective CFA at the location Pz has an estimated amplitude of 0.58 μV. Here, the ratio between the artifact amplitude at the scalp compared with the field strength at the chest level is 0.0015, i.e. essentially smaller than 1%. Therefore, CFA effects of less than 0.04 μV in the scalp potentials during the low-CFA segment (differences in field magnitude <40 μV) should be considered. In addition, the possibility of distortion of the scalp potentials caused by the linked earlobe reference used here was considered. However, an inspection of the data revealed that the amplitude differences between the earlobe channels did not exceed 0.5 μV at any time during the low-CFA segment. Therefore, pulse artifacts at the earlobe electrodes can be excluded.

The upper parts of Figs. 1 and 2 show scalp potentials in 5 parietally-located EEG channels (T5, P3, Pz, P4, T6). The CFA is dominant in all channels. However, besides the CFA, an additional potential can be seen in the low-CFA segment (shaded area and, in more detail, Fig. 2). It is distinct at the parietal locations. It has a positive peak at a latency of about 480 ms and a transient amplitude of about 0.5 μV at Pz.

The topographic distribution of the potential is shown as brain maps in Fig. 3.

The brain map at the top represents the topography of the potential between 350 ms and 480 ms (corresponding to s1–s2). The circumscribed location of the potential over the parietal region of the scalp can be seen. The transient amplitude has a magnitude of 0.5 μV for the parietal positions P3, Pz and P4. Moreover, different potential components are recognizable in the marginal regions of the map (positive (red) over the right hemisphere, negative (blue) over the left). They are caused by the residual cardiac field. They are still dominant at the 4 marginal electrode positions Ad1, Ad2 (over the left and right cheek-bones respectively) and Ad3, Ad4 (halfway between the inion and the left earlobe and halfway between the inion and the right earlobe, respectively).

An analogous brain map for the descending slope of the potential, computed for the interval from 480 ms (peak) to 650 ms is shown in Fig. 3, center. Here, negative transient amplitudes at the parietal locations and positive transient amplitudes at precentral electrodes can be seen.

The low-CFA segment is a temporal window through which the potential can be observed almost undisturbed. We hypothesize that the potential extends beyond this window. This is supported by the brain map shown in Fig. 3, bottom: here, the transient amplitudes were measured between the peak of the potential at 480 ms and a sampling point 50 ms after the R-peak (corresponding to s0–s2).

A different view of the observational data is provided from a statistical perspective. The individually-determined transient amplitudes between s1 and s2 and between s0 and

Table 1

Statistical parameters of individually-determined sampling times (ms after the R-peak of the ECG, $n = 12$)

	s0	s1	s2	s3
Mean	59.17	351.75	476.50	700.00
Standard deviation	9.87	12.04	13.78	1.00
Minimum	39.00	322.00	439.00	698.00
Maximum	70.00	362.00	495.00	702.00

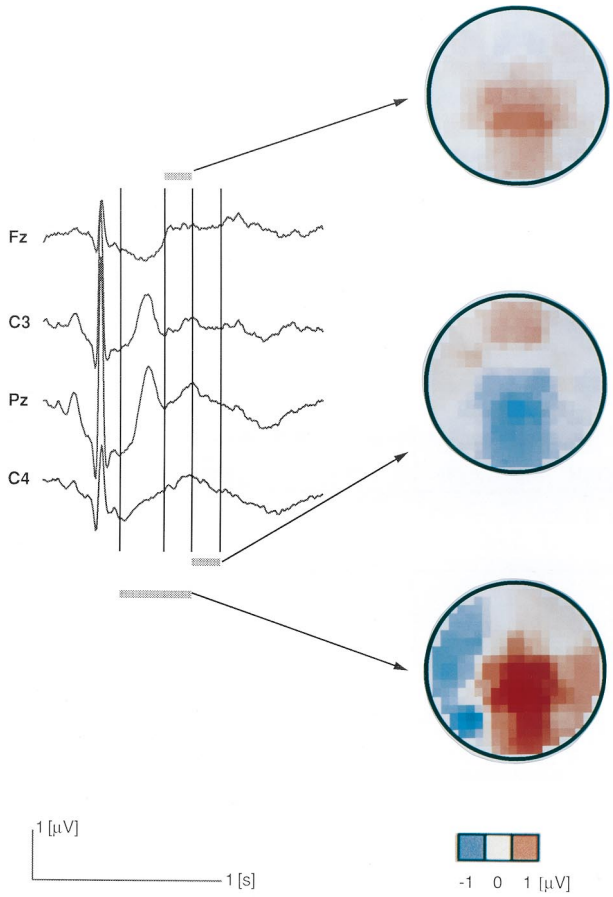

Fig. 3. Topographic distributions of scalp potentials. Top: transient amplitudes between 350 and 480 ms. Center: transient amplitudes between 480 and 650 ms. Bottom: transient amplitudes between 50 and 480 ms. Red: positive potential amplitudes, blue: negative potential amplitudes.

s2 in all channels were analyzed. Distributions of the transient amplitudes centered around 0 μV indicate the absence of potential components, whereas distributions with means deviant from 0 indicate the presence of heart action-related potentials. Wilcoxon tests were carried out (for two samples and 26 channels, i.e. 52 tests). Considering the existing statistical dependencies between the two samples of measurements (s0–s2 and s1–s2) and between different channels, and the fact that the hypothesis was formulated a posteriori, only a descriptive rather than confirmative argument can be derived from the test results (Table 2).

Table 2

Ratio of the number of Wilcoxon tests yielding probabilities <0.005 to the number of tests performed (%)

Electrode site	s1–s2	s0–s2
Frontal	14	0
Centro-temporal	33	33
Parieto-occipital	100	89
Marginal	0	0

Two tests were performed for each channel (s1–s2 and s0–s2). Results for 4 sets of electrode positions: frontal site (7 channels): Fp1, Fp2, F7, F3, Fz, F4, F8; centro-temporal (6 channels): A1, T3, C3, C4, T4, A2; parieto-occipital site (7 channels): T5, P3, Pz, P4, T6, O1, O2; marginal site (4 channels): Ad1, Ad2, Ad3 and Ad4.

Only one of the 14 tests for the frontally-located electrode positions was significant (F8, s1–s2). One-third of the 12 tests for the positions located along the centro-temporal line (T3, C3, C4, T4) were significant (C3, C4 for s0–s2 and s1–s2). In distinct contrast is the finding of 17 significant results in 18 tests for the parieto-occipitally-located channels. These results support the hypothesis of a potential, focused over the parieto-occipital brain regions. Its amplitude (mean = 0.5 μV) has a lower confidence limit of 0.3 μV at the location Pz.

The reliability of the observed potential is illustrated by the data from the experiments in part 2 (GA2, Fig. 4).

The potential courses closely resemble those in Fig. 1. Yet, some differences are obvious, e.g. a prolonged QT segment (313 ms in GA2 compared with 284 ms in GA1) resulting from a lower average heart-beat frequency in part 2. Due to the prolonged QT segment, the low-CFA segment is shifted to later latencies in part 2. (Note that the shaded

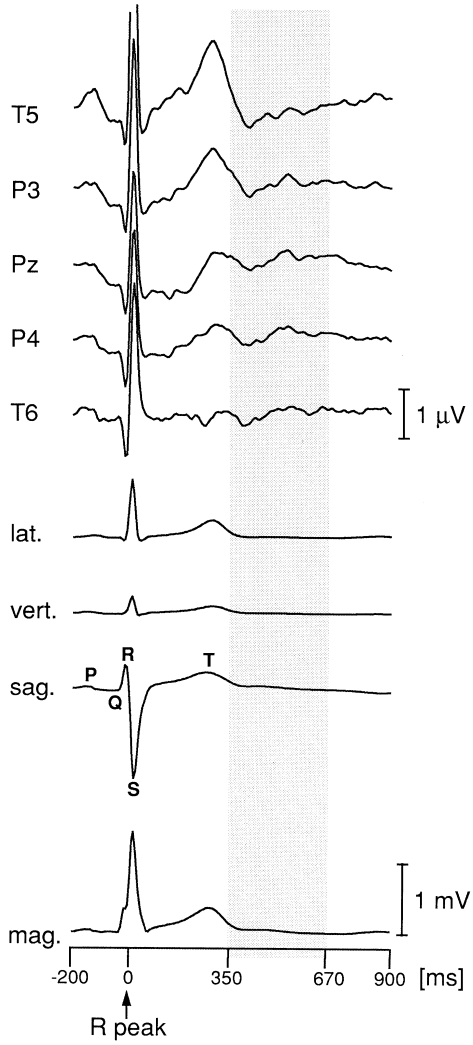

Fig. 4. Grand average, GA2, of scalp potentials in part 2 of the study, analogous to Fig. 1.

area in Fig. 4 representing the low-CFA segment in GA1 partly overlaps with the descending slope of the T-wave of GA2.)

4. Discussion

The main result of the present study is the demonstration of a heart action-related scalp potential over the parietal brain regions, which, according to our knowledge, has not been described before. The positive potential is found topographically circumscribed with a peak amplitude of about 0.5 μV at 480 ms after the R-peak (e.g. channel Pz). The spatial and temporal distributions of the potentials of the 22 subjects were basically similar so that the grand averages provide prototypical pictures of the potential. The statistical analysis, and particularly the experimental replication of the results, support the existence of this potential.

The approach chosen here, of measuring transient amplitudes during individually-determined segments of the cardiac cycle, where only negligibly small effects from the cardiac electrical field are present, yields results undistorted by the CFA, the most important source of artifacts in heart action-related EEG averaging.

Possible influences from other heart action-synchronous events on the scalp potentials were excluded as far as possible by strict adherence to experimental conditions. We had, for example, detected marked reproducible multiphasic potentials topographically circumscribed over the occipital scalp region in some pilot experiments when the subjects had leant their heads against a head support or used a neck roll to stabilize their head position. These pilot observations are not included in the samples of the present study. None of the subjects in the samples showed artifacts of this kind. This observation underscores the need for careful control of heart action-synchronous events that are likely to generate heart action-related EEG artifacts. However, experimental control is only possible for a limited number of variables. In particular, influences from heart action-related non-neural intracranial events cannot be ruled out completely given the current state of knowledge. For example, it is not known whether pulse wave-induced mechanical pulsations of the intracranial structures (Schroth and Klose, 1992) are free from electrical side effects on the EEG. However, the focal parietal location of the potential discussed here favors a neurogenic rather than a pulsation-related origin. Nevertheless, conclusions on brain electric potentials should be drawn from the results presented here with caution.

Another aspect of the results, apart from the parietal potential needs to be discussed. The brain maps show, and the statistical analysis confirms, the absence of a heart action-related potential over the frontal scalp regions. This result is in contradiction of the finding of a frontally-located positive potential described in some of the recent studies mentioned above (e.g. Schandry and Montoya, 1996).

As the potential described here is restricted to the parietal region, where the somatosensory representation areas are located, the presence of somatosensory-evoked components in the observed potential appears likely. As outlined above, a variety of heart action-related events can be regarded as candidate stimuli for the generation of such heart action-related evoked potentials. According to the model of a shower of heart action-related afferent signals outlined above, the observed potential could result from the superposition of small effects from multiple evoked processes triggered at different latencies.

It is an open question whether the potentials obtained by heart action-related EEG averaging also contain other evoked components such as components rooted in visceral heart action-related neuronal signals. In this respect, our results do not yield supportive evidence for the hypothesis that visceral signals transmitted to frontal cortical structures underlie heart action-related potentials (cf. Schandry and Montoya, 1996). The goal of identifying the basal neuronal mechanisms and the pathways lies beyond the abilities of the event-related EEG averaging approach pursued here. This approach is restricted to a phenomenological level of description of electrical brain activity and cannot, therefore, alone, yield convincing arguments for a decision between competing neuronal hypotheses. In any case, further research will be necessary to determine whether the observed potentials are pure evoked brain potentials.

Acknowledgements

We thank T. Pollmacher for stimulating and constructive comments on this research and the manuscript and Ms. P. Fosbury for linguistic support in writing the paper.

References

Cervero, F. and Foreman, R.D. Sensory innervation of the viscera. In: A.D. Loewy and K.M. Spyer (Eds.), Central Regulation of Autonomic Functions. Oxford University Press, New York, 1990, pp. 104–125.

Chen, A.C.N. and Dworkin, S.F. Human pain and evoked potentials: possible assessment of headache with endogenous brain potentials triggered by the R wave of EKG in pain patients. In: J. Courjon, F. Mauguiere and M. Revol (Eds.), Advances of Neurology: Clinical Application of Evoked Potentials in Neurology, Vol. 32. Raven Press, New York, 1982, pp. 389–395.

Dirlich, G., Vogl, L., Plaschke, M. and Strian, F. Cardiac field effects on the EEG. Electroenceph. clin. Neurophysiol., 1997, 102: 307–315.

Gratton, G., Coles, M.G.H. and Donchin, E. A new method for off-line removal of ocular artifact. Electroenceph. clin. Neurophysiol., 1983, 55: 468–484.

Jänig, W. Neurobiology of visceral afferent neurons: neuroanatomy, functions, organ regulations and sensations. Biol. Psychol., 1996, 42 (1,2): 29–51.

Jasper, H. The ten twenty electrode system of the international federation. Electroenceph. clin. Neurophysiol., 1958, 10: 371–375.

Jones, G.E., Leonberger, T.F., Rouse, C.H., Caldwell, J.A. and Jones, K.R. Preliminary data exploring the presence of an evoked potential asso-

ciated with cardiac visceral activity. Psychophysiology, 1986, 23: 445 (abstract).

Jones, G.E., Jones, K.R., Rouse, C.H., Scott, D.M. and Caldwell, J.A. The effect of body position and the perception of cardiac sensations: an experiment and theoretical implications. Psychophysiology, 1987, 24: 300–311.

Jones, G.E., Rouse, C.H. and Jones, K.R. The presence of visceral evoked potentials elicited by cutaneous palpation of heartbeats in high and low awareness subjects. Psychophysiology, 1988, 25: 459 (abstract).

Montoya, P., Schandry, R. and Mueller, A. Heartbeat evoked potentials (HEP): topography and influence of cardiac awareness and focus of attention. Electroenceph. clin. Neurophysiol., 1993, 88: 163–172.

Paintal, A.S. Cardiovascular receptors. In: E. Neil (Ed.), Handbook of Sensory Physiology (Vol. III/I): Enteroceptors. Springer–Verlag, Berlin, 1972.

Reed, S.D., Harver, A. and Katkin, E.S. Interoception. In: J.T. Cacioppo and L.G. Tassinary (Eds.), Principles of Psychophysiology. Physical, Social, and Inferential Elements. Cambridge University Press, Cambridge, 1990.

Riordan, H., Squires, N.K. and Brener, J. Cardio-cortical potentials: electro-physiological evidence for visceral perception. Psychophysiology, 1990, 27: 59 (abstract).

Schandry, R. and Montoya, P. Event-related brain potentials and the processing of cardiac activity. Biol. Psychol., 1996, 42: 75–85.

Schandry, R., Sparrer, B. and Weitkunat, R. From the heart to the brain: a study of heartbeat contingent scalp potentials. Internat. J. Neurosci., 1986, 30: 261–275.

Schroth, G. and Klose, U. Cerebrospinal fluid flow. I. Physiology of cardiac related pulsation. Neuroradiology, 1992, 35: 1–9.